Journal of Modern Researches on Electronic Defense Systems

Receive: 1 May 2025 Accept: 3 August 2025

Super Wide Band Multiple-Input Multiple-Output Antenna for UWB Applications with Dual Band-Notched Characteristics

Farzad Mohajeri[1*], Faezeh Bahmanzadeh[2]

[*]Corresponding Author: mohajeri@shirazu.ac.ir

[1,2] Department of Communications and Electronics, School of Electrical and Computer Engineering, Shiraz University, Shiraz, Iran.

Abstract – *This paper presents a compact dual-band-notched super wide band (SWB) multiple-input multiple-output (MIMO) antenna for UWB applications. The bandwidth of the antenna is near 38 GHz from 2.3 to 40 GHz, which covers L, S, C, X, Ku, K, and Ka bands and has two notched frequencies around 3.1-3.7 GHz for WiMAX and 5.1-5.8 GHz for WLAN. This antenna comprises two identical elements, fed by two 50 Ω microstrip lines and placed adjacent on a low-cost FR-4 substrate. The total size of the antenna is about 31 × 65 × 1.6 mm^3. To suppress the interferences of WiMAX and WLAN bands, two elliptic single complementary split-ring resonators (ESCSRRs) were etched out of the radiating patch and to achieve a good isolation between the two elements a long vertical open-ended slot is etched out of the shared ground plane and an isolation of more than 17 dB is achieved. In addition, the Envelope Correlation Coefficient (ECC) value is less than 0.01.*

Keywords: *Band-notched characteristics, elliptic single complementary split-ring resonators (ESCSRRs), MIMO antennas, super wide band (SWB) antennas, UWB Applications.*

1. Introduction

Multiple-input multiple-output (MIMO) technology has been developed over many years and has become very popular due to its special characteristics, like a significant increase in capacity of UWB systems without the need for additional frequency range and data transmission efficiency. In addition, MIMO systems can mitigate signal fading due to the multipath that occurs during a wireless transmission. Therefore, the reception's quality and reliability are improved [1]. UWB technology has also drawn much attention since the Federal Communications Commission (FCC) allocated the unlicensed frequency spectrum from 3.1 to 10.6 GHz [2]. Besides lots of interesting characteristics of UWB technology, such as high precision ranging and low power spectral density, it also has some problems, such as multipath fading and reliability limitations, which the convergence of MIMO and UWB technology can overcome these issues [3]. However, the UWB frequency range interferes with existing narrowband communication systems such as worldwide interoperability for microwave access (WiMAX), C-band, wireless local area network (WLAN), and X-band satellite communication. As regards this point, antennas with band-notched characteristics need to cancel the mentioned interfering frequency bands, and several investigations have been conducted in this field over many years. For instance, in [4] and [5], two UWB antennae are proposed with single-notched bands at WiMAX and WLAN, respectively. To suppress these frequency bands, an inverted-π model slot and an open stub have been reduced from the radiating patches. Antennas with dual and triple band-notched characteristics are also introduced in [6], [7], and [8], respectively. In [9] and [10], different types of split-ring resonators are etched on the radiating patch, and in [11], three open-ended slots are introduced into the radiating patch to filter WiMAX, WLAN, and X-band interferences. In [12], a monopole antenna with six band-notched characteristics is presented based on SRRs and U-shaped parasitic strips, and notched bands around 2.96-3.33 GHz, 3.73-3.88 GHz, 4.43-4.53 GHz, 5.37-5.57 GHz, 7.02-7.30 GHz, and 7.56-8.06 GHz have been obtained.

Portable devices with limited space require compact MIMO antennas, and by placing the elements near each other, mutual coupling will increase extremely; therefore, designing compact MIMO antennas with low mutual

coupling has become a challenging issue. For example, in [13-15], elements of the MIMO antennas are placed orthogonal to each other, and the diversity causes high isolation of more than 15 dB, 20 dB, and 20 dB for each antenna. In [16] and [17], the mutual coupling is reduced by placing two inverted L-shaped stubs into the shared ground plane, and an isolation of more than 20 dB and 17 dB is obtained in each case. In [18] and [19], substrate integrated waveguide (SIW) structures have been utilized to reduce mutual coupling, and in [20] and [21], an electromagnetic band gap (EBG) structure has been utilized to reduce mutual coupling to less than -25 dB and to enhance impedance bandwidth, respectively. Furthermore, in [22], a quad-element band-notched UWB MIMO antenna is proposed with an overall size of 60 × 60 mm^2 and covers a bandwidth ranging from 2.73 to 10.68 GHz. A mushroom-like EBG structure is used to reduce the interference of WLAN, also the mutual coupling between the elements is less than -15 dB. In [23], a dual band-notched MIMO antenna is proposed with a total size of 25×39 mm^2 and impedance bandwidth from 2.6 to 12.5 GHz. In this work, to reduce mutual coupling to less than -20 dB, the elements are placed perpendicular to each other, and to filter the interferences of WLAN and X-band, two L-shaped slots are etched on each radiating patch. Among different kinds of metamaterials, near zero-index metamaterial (NZIM), is of special interest. NZIM can collimate the diverging waves into plane waves. This collimation property increases the directivity and gain of the antenna [10]. So, it is worth combining the concept of fractal structures with the linear antenna array, while using the benefits of NZIM configurations.

This research investigates a compact SWB 2-element MIMO antenna with band-notched characteristics. The total size of this design is 31 × 65 × 1.6 mm^3, which is small compared to some previous research [24] and consists of two identical monopole antennas with circular patches placed next to each other at a distance of 21 mm and fed by two 50 Ω microstrip lines. To enhance the bandwidth of the antenna, two large elliptic slots are etched out of the shared ground plane, and a bandwidth of more than 178% is achieved from 2.3 to 40 GHz, which covers L, S, C, X, Ku, K, and Ka bands for each port. Mutual coupling between two ports is reduced by introducing a long rectangular open-ended slot into the shared ground plane between the two similar elements, and an isolation of more than 17 dB is achieved. Each element separately is a single-input single SWB antenna with dual band-notched characteristics, having the size of 31 × 31 × 1.6 mm^3. To reduce the interference of WiMAX and WLAN frequency bands, two ESCSRRs of different dimensions are etched on each radiating patch, and their location is optimized using the HFSS simulator package. The designed MIMO antenna provides an omnidirectional radiating pattern at the xoz plane and nearly 6 dBi of peak gain. Also, the value of *ECC* is less than 0.01.

2. Antenna Design Procedure

2.1 Single Element

Reference antenna with a total size of 31 × 31 × 1.6 mm^3 consists of a circular patch fed by a 50 Ω microstrip line and placed on the top side of the substrate with a defected ground plane, which is placed on the bottom side of the substrate, is designed in iteration 1 as given in Figure 1 (a). A large elliptic slot having a major radius of D1 = 30 mm and a minor radius of D2 = 23 mm is introduced into the ground plane to enhance the bandwidth of the antenna by about 30 GHz. This slot is a key point of having a super wide impedance bandwidth from 2 to 40 GHz.

Two quarter-wavelength ESCSRRs of different dimensions are etched on the radiating patch to filter the interferences of WiMAX and WLAN bands. The proper length of the ESCSRRs can be obtained from the following equation, and their location has been optimized [10].

$$L = K\pi(0.5D_{min} - w) - g \approx \frac{\lambda_g}{4} = \frac{c}{4f_{Notch}\sqrt{\varepsilon_{eff}}} \quad (1)$$

Where L is the total length of the elliptic slots, which should be approximately equal to a quarter wavelength at the desired notch frequencies. K is equal to the ratio of D_{max}/D_{min} and w is the thickness of each ESCSRRs, f_{Notch} is the central frequency of the notched bands and c is the speed of light in free space, also ε_{eff} can obtain from the following equation [10].

$$\varepsilon_{eff} = \frac{\varepsilon_r+1}{2} + \frac{\varepsilon_r-1}{2}\left(1 + \frac{12h}{w_f}\right)^{-\frac{1}{2}} \quad (2)$$

Where ε_r is the relative permittivity of substrate that is 4.4 for FR-4, h is the thickness of the substrate which is 1.6 mm in this case, and w_f is the width of the microstrip feed line which is about 2.8 mm, respectively. By introducing the designed ESCSRRs on the radiating patch of the designed antenna in Iteration 1, a monopole SWB antenna is designed in iteration 2 ,having a super wide impedance bandwidth of about 178% from 2.3 to 40 GHz except at the two notched frequency bands. The larger ESCSRR having a total length of 10.34 mm reduces the interferences of WiMAX from 2.89 to 3.84 GHz, and the smaller ESCSRR ,having a total length of 7.59 mm, filters the WLAN frequency range at center frequencies of 3.6 GHz and 5.7 GHz respectively. Figure 1 (b) shows the configuration of the SISO ddual-band-notchedantenna and Figure 1 (c) shows the ESCSRRs in detail. S_{11} characteristics of iterations 1 and 2 are compared in the following section.

2.2 MIMO Antenna

The two designed elements MIMO antenna are shown in Figure 2. The total dimensions of the antenna are about 31 × 65 × 1.6 mm^3 using the SWB band-notched elements presented in the previous section. Each element consists of a circular patch having a radius of 7 mm and a defected ground plane. The identical SWB monopoles are placed next to each

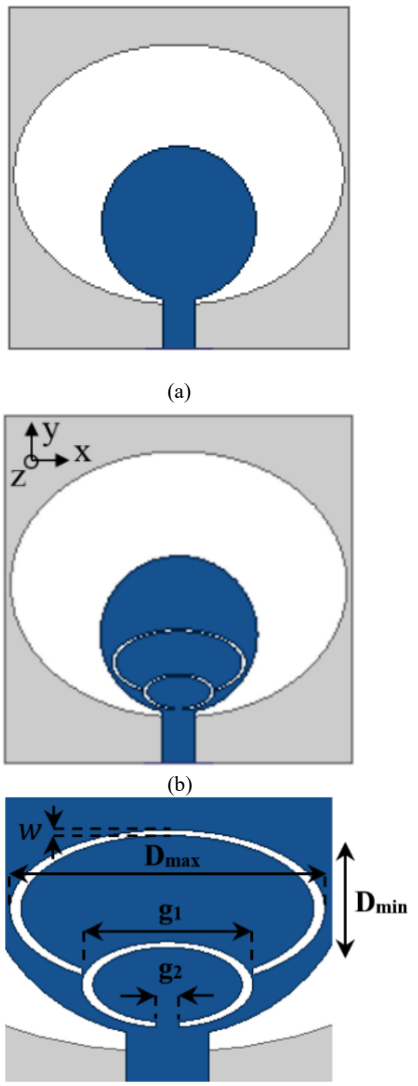

Figure 1. Geometry of the designed SISO antenna. (a) iteration 1, (b) iteration 2, (c) ESCSRRs on the patch

other, and the distance between the centers of the two patches is about 27 mm. Therefore, a super-wide impedance matching can be achieved. To reduce the mutual coupling between the elements of the antenna, an open-ended rectangular slot having the size of $W_s \times L_s$ is etched out of the shared ground plane. The final optimum dimensions are given in Table 1. It is worth noting that the parameters of ESCSRRs on the antenna patch have the greatest impact on the antenna characteristics.

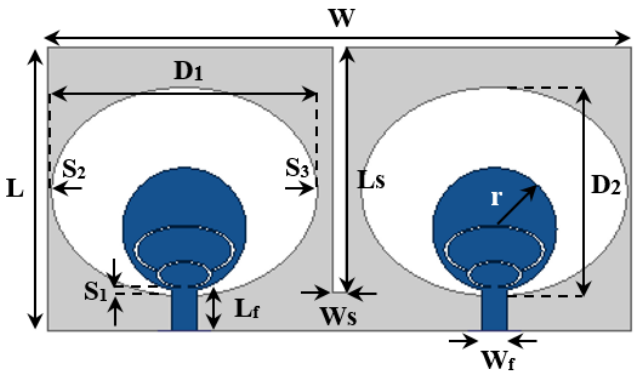

Figure 2. Geometry of the designed MIMO antenna

Table 1. Final optimum dimensions of the designed MIMO antenna

Parameters	Dimension (mm)	Parameters	Dimension (mm)
W	31	***Wf***	3
L	66	***Lf***	5
D1	30	***S1***	0.6
D2	23	***S2***	0.5
WS	1.5	***S3***	1.75
LS	27.8	***g1***	6.2
Dmax	11.4	***g2***	0.84
Dmin	8.4	***r***	7

To elaborate on the role of ESCSRRs on radiating patches, the simulated surface current distribution of the designed MIMO antenna is shown in Figure 3 at notched central frequencies when port 1 is exited and port 2 is terminated by a 50 Ω matched load and as is clear in this figure, current distribution perturbed by the presence of ESCSRRs. Figure 3 (a) depicts the current distribution at 3.6 GHz. In this figure, the concentration of surface currents is around the larger ESCSRR, which filters the WiMAX frequency band, and Figure 3 (b), shows surface currents at 5.7 GHz. similarly, the concentration of surface currents is around the smaller ESCSRR. Also, it is evident from this figure that the mutual coupling among the elements is small, and hence, the proposed MIMO antenna has good isolation.

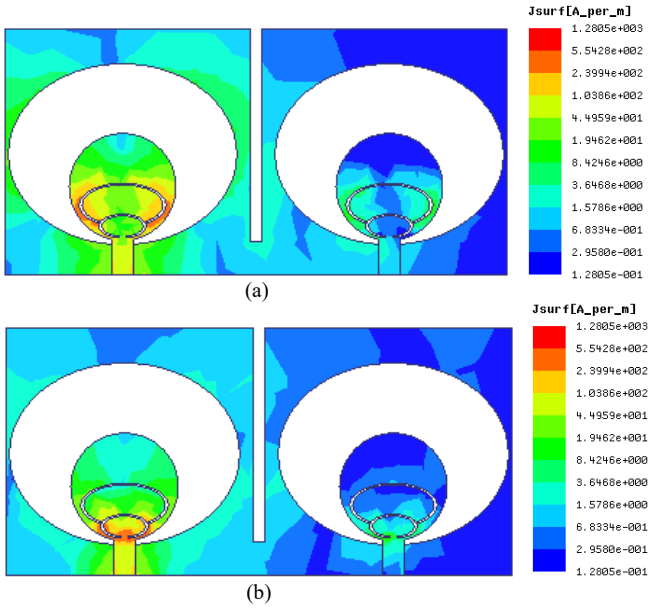

Figure 3. Surface current distribution of the designed MIMO antenna at (a) 3.6 GHz, (b) 5.8 GHz

3. Full-Wave Simulation Results

S-parameters of the designed antennas named iterations 1 and 2 are compared in Figure 4. It is clear from this figure that the single-element designed antenna in iteration 1 can provide a super wide impedance bandwidth ($|S_{11}|$ less than -10 dB) from 2.4 to 40 GHz and covers L, S, C, X, Ku, K, and Ka bands. Also, iteration 2 covers the entire bandwidth from 2.3 to 40 GHz with two notches around 2.89 to 3.84 GHz for WiMAX and 5.16 to 6.1 GHz for WLAN. Figure 5 indicates the magnitudes of the simulated S-parameters S_{11}, S_{22}, and S_{12} for the designed MIMO antenna. Each port can cover the impedance bandwidth from 2.3 to 40 GHz with two notches from 2.9 to 3.9 GHz and 5 to 6.1 GHz for port 1 and from 2.9 to 4.2 GHz and 5.1 to 6.3 GHz for port 2 for WiMAX and WLAN, respectively. Also, S_{12}, which represents the mutual coupling between two elements, is less than -17 dB in the entire operating band, and isolation is very high at 17 and 37.7 GHz.

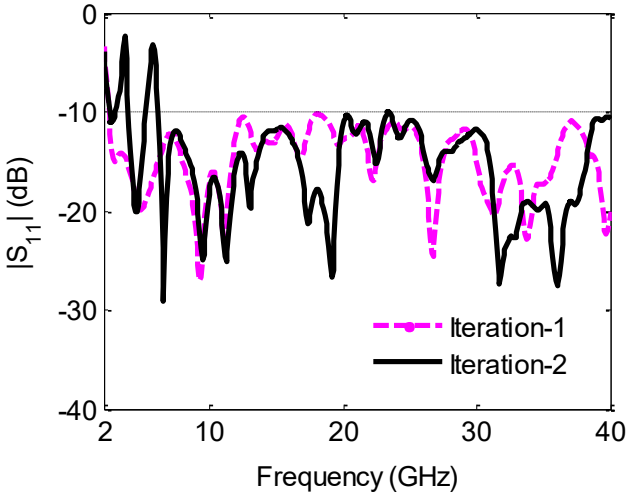

Figure 4. Simulated reflection coefficient of the SISO-designed antennas

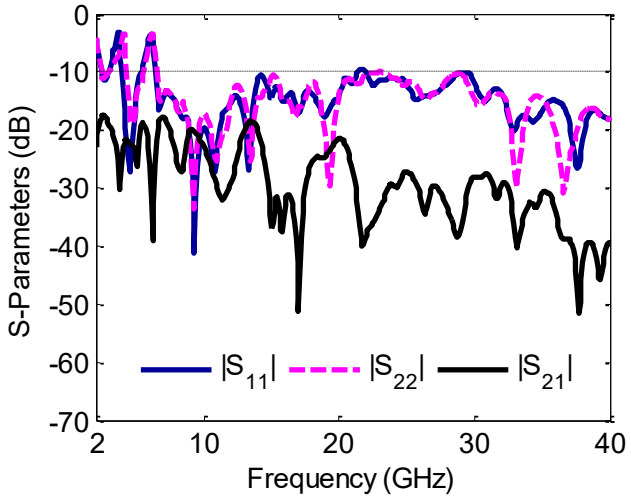

Figure 5. S-Parameters of the designed MIMO antenna

The antenna radiation patterns at 3, 10, and 18 GHz have been observed in Figure 6 in both xoz and yoz planes when port 1 is excited and port 2 is terminated by a 50 Ω matched load and vice versa. As shown in this figure, the proposed MIMO antenna radiates omnidirectional and bidirectional patterns in the xoz and yoz planes, respectively. Achieving a pure omnidirectional radiation pattern over the complete SWB band is a challenging task however, the antenna provides a quasi-omnidirectional pattern in the xoz plane at the mentioned frequencies. The simulated peak gain for ports 1 and 2 is shown in Figure 7. It can be observed that the peak gain decreases sharply at notch frequencies. A peak gain of 8.8 dBi is achieved for each port.

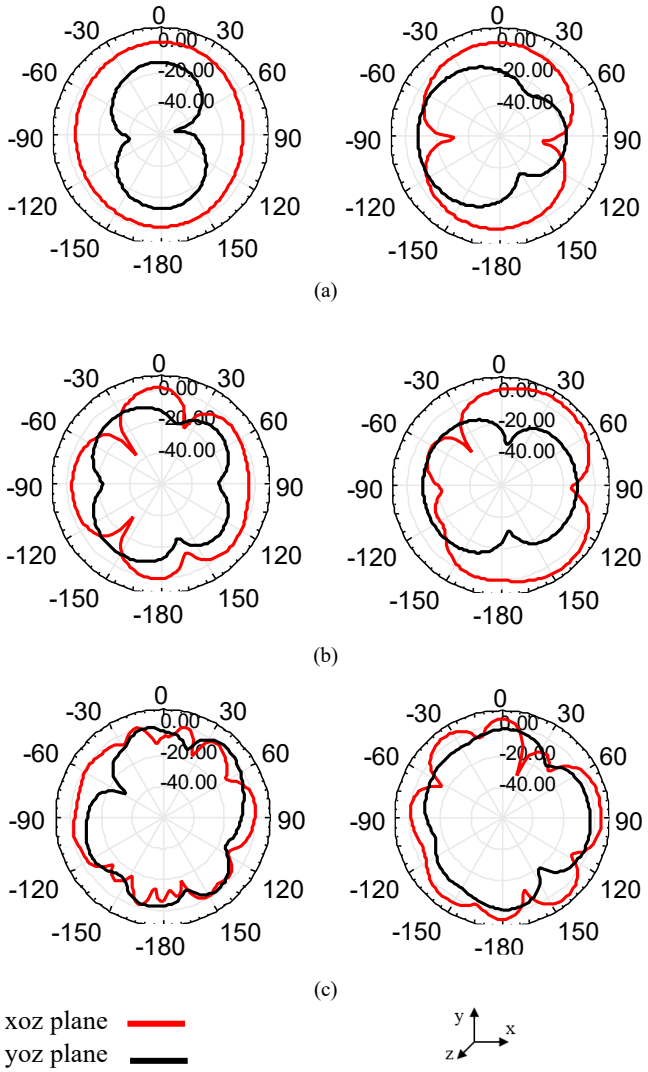

Figure 6. Radiation patterns of the designed MIMO antenna for each port when port 1 is exited and port 2 is matched (left) and when port 2 is exited and port 1 is matched (right) at (a) 3 GHz, (b) 10 GHz, (c) 18 GHz

MIMO performance characteristics such as Envelope Correlation Coefficient (*ECC*) and multiplexing efficiency (η_{mux}) of the suggested MIMO antenna can be obtained from equations 3, [25] and 4, [26] respectively.

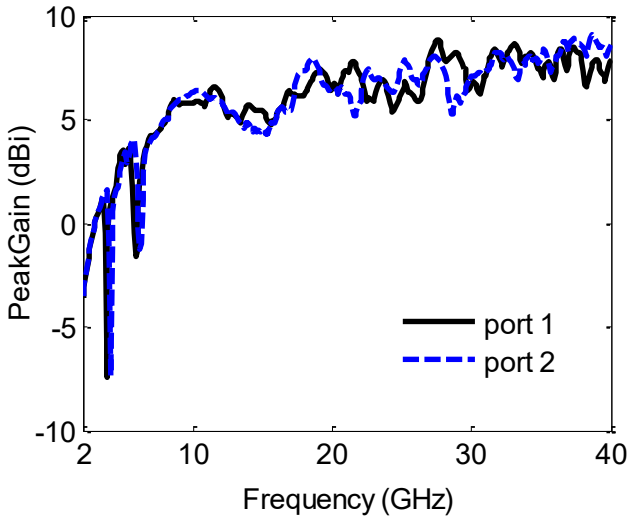

Figure 7. Simulated peak gain of the designed MIMO antenna for each port

$$ECC = \frac{|S_{11}^{*}S_{21}+S_{21}^{*}S_{22}|^2}{(1-(|S_{11}|^2+|S_{21}|^2))(1-(|S_{22}|^2+|S_{21}|^2))} \quad (3)$$

Where S_{11} and S_{22} are the reflection coefficients of the two ports and S_{12} and S_{21} are the couplings between the two ports.

$$\eta_{mux} = \sqrt{\eta_1\eta_2(1-|r|^2)} \quad (4)$$

Where η_1 and η_2 are the total efficiencies of port 1 and port 2, respectively, and $|r|^2$ is the square root of the magnitude of the complex correlation between the two elements of the MIMO antenna, and it is almost equal to *ECC*. Simulated multiplexing efficiency and *ECC* of the MIMO antenna are plotted in Figure 8. To have an uncorrelated MIMO antenna, the *ECC* value should be less than 0.5, and as it is clear from Figure 8, the *ECC* value of the proposed MIMO antenna is less than 0.01, which is significant. Also, multiplexing efficiency is above -4 dB throughout the whole operating bandwidth.

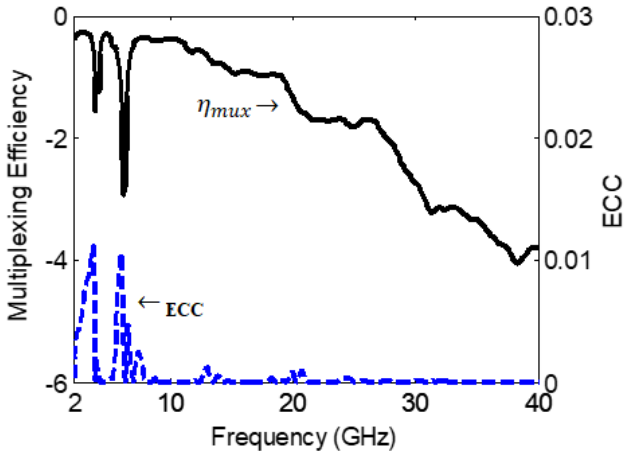

Figure 8. Simulated multiplexing efficiency and *ECC* versus frequency

Table 2 shows the comparison of the characteristics of the antenna proposed in this paper with some similar antennas. In this table, parameters such as dimensions, bandwidth, multiplexing efficiency, isolation and Envelope Correlation Coefficient are compared. It is observed that the antenna proposed in this paper is superior to other antennas in every aspect.

Table 2. Comparison of the proposed antenna with some similar antennas

ECC	Isolation (dB)	Multiplexing Efficiency	Band Width (GHz)	Dimension (mm^2)	Ref.
>0.02	>16	-	2.8-11.6	26×26	[4]
>0.18	>15	>9.9	2.73-10.68	60×60	[22]
>0.15	>16	>8.5	2.8-11.2	39×25	[23]
>0.01	>17	>4	2.3-40	65×31	**This work**

4. Conclusion

In this paper, a dual-band-notched SWB MIMO antenna is presented. The total size of the antenna is 31× 65 × 1.6 mm^3 covering 28.7 GHz impedance bandwidth from 2.3 to 40 GHz at each port except at the two notched bands from 2.9 to 3.9 GHz for WiMAX (3.3-3.7GHz) and 5 to 6.1 GHz for WLAN (5.1-5.825GHz) which appears in the existence of two ESCSRRs on the two radiating patches. To reduce the mutual coupling between two adjacent elements, an open-ended rectangular slot is etched on the shared ground plane, and an isolation of more than 17 dB is obtained. The presented antenna provides a peak gain of about 8.8 dBi, *ECC* of less than 0.01, multiplexing efficiency above -4 dB, and a nearly omnidirectional radiating pattern in the entire working band.

References

[1] G. Casu, L. Tuta, I. Nicolaescu, and C. Moraru, "Some aspects about the advantages of using MIMO systems," *in 2014 22nd Telecommunications Forum Telfor (TELFOR)*, Belgrade, Serbia, pp. 12-17, November 2014, Doi: 10.1109/TELFOR.2014.7034415.

[2] Federal Communications Commission (FCC), Revision of Part 15 of the Commission's Rules Regarding Ultra-Wideband Transmission Systems First Rep. and Order, ET Docket 98-153, FCC 02-48, Adopted: Feb. 2002; Released, Apr. 2002.

[3] J. Jervase-Yak and A. H. Al-Shamsi, "MIMO Antenna for UWB Communications," *International Journal of Communications, Network and System Sciences*, vol. 9,

no. 5, pp. 177-183, May 2016, Doi: 10.4236/ijcns.2016.95017.

[4] R. Sanmugasundaram, N. Somasundaram, and R. Rengasamy, "Ultrawideband Notch Antenna with EBG Structures for WiMAX and Satellite Application," *Progress in Electromagnetics Research Letters*, vol. 91, pp. 25-32, April 2020, Doi: 10.2528/PIERL20012903.

[5] A. Dolatkhah and B. Dorostkar, "Analysis of a microstrip antenna with an incomplete ground plane structure that can be used in electronic defense systems," *Journal of Modern Researches on Electronics Defence Systems,* vol. 2, no. 5, pp. 22-27, March 2024, Doi: 10.22034/joeds.2024.445718.1037. (In Persian)

[6] Z. Li, C. Yin, and X. Zhu, "Compact UWB MIMO Vivaldi Antenna with Dual Band-Notched Characteristics," *IEEE Access*, vol. 7, pp. 38696-38701, March 2019, Doi: 10.1109/ACCESS.2019.2906338.

[7] F. Bahmanzadeh and F. Mohajeri, "Simulation and fabrication of a high-isolation very compact MIMO antenna for ultra-wide band applications with dual band-notched characteristics," *International Journal of Electronics and Communications (AEU)*, vol. 128, pp. 153505, 2021, Doi: 10.1016/j.aeue.2020.153505.

[8] M. Sharma, Y. K. Awasthi, and H. Singh, "Design of CPW-Fed High Rejection Triple Band-Notch UWB Antenna on Silicon Substrate with Diverse Wireless Applications," *Progress in Electromagnetics Research C*, vol. 74, pp. 19-30, May 2017, Doi: 10.2528/PIERC16092101.

[9] S. Lakrit, S. Das, S. Ghosh, and B. T. P. Madhav, "Compact UWB flexible elliptical CPW-fed antenna with triple notch bands for wireless communications," *International Journal of RF and Microwave Comput-Aided Engineering*, vol. 30, no. 7, pp. 1-14, February 2020, Doi: 10.1002/mmce.22201.

[10] D. Sarkar, K. V. Srivastava, and K. Saurav, "A Compact Microstrip-Fed Triple Band-Notched UWB Monopole Antenna," *IEEE Antennas and Wireless Propagation Letters*, vol. 13, pp. 396-399, February 2014, Doi: 10.1109/LAWP.2014.2306812.

[11] D. T. Nguyen, D. H. Lee, and H. C. Park, "Very Compact Printed Triple Band-Notched UWB Antenna with Quarter-Wavelength Slots," *IEEE Antennas and Wireless Propagation Letters*, vol. 11, pp. 411-414, April 2012, Doi: 10.1109/LAWP.2012.2192900.

[12] S. Luo, Y. Chen, D. Wang, Y. Lia, and Y. Li, "A monopole UWB antenna with sextuple band-notched based on SRRs and U-shaped parasitic strips," *AEU - International Journal of Electronics and Communications*, vol. 120, pp. 112-119, June 2020, Doi: 10.1016/j.aeue.2020.153206.

[13] S. Syedakbar, S. Ramesh, and J. Deepa, "Ultra-wideband monopole planar MIMO antenna for portable devices," *in 2017 IEEE International Conference on Electrical, Instrumentation and Communication Engineering (ICEICE)*, Karur, India, pp. 1-4, April 2017, Doi: 10.1109/ICEICE.2017.8191961.

[14] L. Liu and T. I. Yuk, "Compact MIMO Antenna for Portable Devices in UWB Applications," *IEEE Transactions on Antennas and Propagation*, vol. 61, no. 8, pp. 4257-4264, May 2013, Doi: 10.1109/TAP.2013.2263277.

[15] J. Ren, W. Hu, Y. Yin, and R. Fan, "Compact Printed MIMO Antenna for UWB Applications," *IEEE Antennas and Wireless Propagation Letters*, vol. 13, pp. 1517-1520, July 2014, Doi: 10.1109/LAWP.2014.2343454.

[16] M. A. Haq and S. Koziel, "Ground Plane Alterations for Design of High-Isolation Compact Wideband MIMO Antenna," *IEEE Access*, vol. 6, pp. 48978-48983, August 2018, Doi: 10.1109/ACCESS.2018.2867836.

[17] E. Thakur, N. Jaglan, and S. D. Gupta, "Design of Compact UWB MIMO Antenna with Enhanced Bandwidth," *Progress in Electromagnetics Research C,* vol. 97, pp. 83-94, November 2019, Doi: 10.2528/PIERC19083004.

[18] B. Niu and J. Tan, "Compact four-element MIMO antenna using T-shaped and anti-symmetric U-shaped slotted SIW cavities," *Electronics Letters*, vol. 55, no. 19, pp. 1031–1032, September 2019, Doi: 10.1049/el.2019.2142.

[19] B. Niu and J. H. Tan, "Compact Two-Element MIMO Antenna Based on Half-Mode SIW Cavity with High Isolation," *Progress in Electromagnetics Research Letters,* vol. 85, pp. 145-149, July 2019, Doi: 10.2528/PIERL19050103.

[20] T. Dabas, D. Gangwar, B. K. Kanaujia, and A. K. Gautam, "Mutual coupling reduction between elements of UWB MIMO antenna using small size uniplanar EBG exhibiting multiple stop bands," *AEU-International Journal of Electronics and Communications*, vol. 93, pp. 32-38, May 2018, Doi: 10.1016/j.aeue.2018.05.033.

[21] H. Babaei, S. A. Gohari, and P. Mohamadi, "Design, Simulation, Fabrication and Determining the Equivalent Circuit Model of a Reconfigurable RFSS Unit Cell Filter for Electromagnetic Protection of Space Payload Systems," *Journal of Space Science and Technology*, vol. 16, no. 4, pp. 71-82, February winter 2024, Doi: 10.30699/jsst.2023.1448. (In Persian)

[22] N. K. Kiem, H. N. B. Phuong, and D. N. Chien, "Design of compact 4x4 UWB MIMO antenna with WLAN band rejection," *International Journal of Antennas and Propagation*, vol. 2014, pp. 539094, July 2014, Doi: 10.1155/2014/539094.

[23] Z. Tang, J. Zhan, X. Wu, Z. Xi, L. Chen, and S. Hu, "Design of a compact UWB-MIMO antenna with high isolation and dual band-notched characteristics," *Journal of Electromagnetic Waves and Applications*, vol. 34, no. 4, pp. 500-513, February 2020, Doi: 10.1080/09205071.2020.1724200.

[24] R. Hussain and M. S. Sharawi, "A Cognitive Radio Reconfigurable MIMO and Sensing Antenna System," *IEEE Antennas and Wireless Propagation Letters*, vol.

14, pp. 257-260, October 2014, Doi: 10.1109/LAWP.2014.2361450.

[25] S. Blanch, J. Romeu, and I. Corbella, "Exact representation of antenna system diversity performance from input parameter description," *Electronics Letters*, vol. 39, no. 9, pp. 705-707, June 2003, Doi: 10.1049/el:20030495.

[26] R. Tian, B. K. Lau, and Z. Ying, "Multiplexing efficiency of MIMO antennas,*" IEEE Antennas and Wireless Propagation Letters*, vol. 10, pp. 183-186, March 2011, Doi: 10.1109/LAWP.2011.2125773.